LAWRENCE
LIVERMORE
NATIONAL
LABORATORY

LLNL-CONF-483351

Verification and validation of CgWind: a high-order accurate simulation tool for wind engineering

K. K. Chand, M. A. Singer

May 9, 2011

13th International Conference on Wind Engineering
Amsterdam, Netherlands
July 10, 2011 through July 15, 2011

Disclaimer

This document was prepared as an account of work sponsored by an agency of the United States government. Neither the United States government nor Lawrence Livermore National Security, LLC, nor any of their employees makes any warranty, expressed or implied, or assumes any legal liability or responsibility for the accuracy, completeness, or usefulness of any information, apparatus, product, or process disclosed, or represents that its use would not infringe privately owned rights. Reference herein to any specific commercial product, process, or service by trade name, trademark, manufacturer, or otherwise does not necessarily constitute or imply its endorsement, recommendation, or favoring by the United States government or Lawrence Livermore National Security, LLC. The views and opinions of authors expressed herein do not necessarily state or reflect those of the United States government or Lawrence Livermore National Security, LLC, and shall not be used for advertising or product endorsement purposes.

Verification and validation of CgWind: a high-order accurate simulation tool for wind engineering

Kyle K. Chand[a] and Michael A. Singer[b]
[a]*Lawrence Livermore National Laboratory, Livermore, CA, USA, chand1@llnl.gov*
[b]*Lawrence Livermore National Laboratory, Livermore, CA, USA, singer3@llnl.gov*

ABSTRACT: This paper presents the verification and initial validation of CgWind, a new, high-fidelity, large eddy simulation code for wind engineering applications. CgWind utilizes fourth-order accurate spatial discretizations of the incompressible Navier-Stokes equations on composite structured grids to achieve both high efficiency and resolution without sacrificing the ability to model complex and moving geometries. Computational models such as CgWind consist of complex numerical algorithms and software whose correctness must be verified prior to their use as a mathematical model for practical simulations. The process of *verification* demonstrates that a numerical model is implemented correctly and confirms the theoretical properties (stability and accuracy) of the discrete approximations of the continuous mathematical model. After successful verification, *validation* then determines the suitability of the mathematical model to capture the relevant physical phenomenon of problems of interest. Rigorous verification has been built into the development of CgWind, and verification of accuracy and convergence has been demonstrated. The code is now undergoing validation by comparison to experimental data.

1 INTRODUCTION

CgWind is a new, high-fidelity simulation tool designed to meet the modeling requirements of advanced wind engineering applications. The tool couples large eddy simulation (LES) models, based on the incompressible Navier-Stokes equations, with moving grid techniques designed resolve the flow near bodies in relative motion such as turbine blades (Chand et al., 2010). While initially intended for wind energy problems, CgWind is a useful general purpose wind engineering simulation tool. Currently under development at Lawrence Livermore National Laboratory, CgWind will be a freely available tool for use by wind engineers, researchers and the general wind engineering community.

Verification and validation of CgWind is a necessary precursor to its successful use as an actual wind engineering tool. Verification is the process whereby the algorithms and implementation of CgWind are shown to be correct. For complex mathematical models that are applied in complex geometries, verification is nontrivial. However, CgWind is implemented using the Overture framework, which provides an extensive infrastructure for the verification of numerical techniques using manufactured solutions (Chand and Henshaw, 2007). Rigorous verification is therefore incorporated into CgWind's development process. Once a numerical method is verified, the validation of the mathematical model can begin. Validation of the code is accomplished using experimental data relevant to wind engineering applications. This talk will present the techniques used to verify CgWind's numerical methods and to validate its mathematical models.

2 NUMERICAL APPROACH FOR THE NAVIER-STOKES EQUATIONS

CgWind solves the incompressible Navier-Stokes (INS) equations with a pressure-velocity formulation and a split-step method where the pressure is computed in a separate step. For a given domain Ω, with boundary $\partial\Omega$, the governing equations are

$$\begin{aligned} \mathbf{u}_t + (\mathbf{u}\cdot\nabla)\mathbf{u} + \nabla p - \nu\Delta\mathbf{u} - \mathbf{f} = 0, &\qquad t>0, \quad \mathbf{x}\in\Omega \\ \Delta p + \nabla\mathbf{u} : \nabla\mathbf{u} - \alpha\nabla\cdot\mathbf{u} - \nabla\cdot\mathbf{f} = 0, &\qquad t>0, \quad \mathbf{x}\in\Omega \end{aligned} \tag{1}$$

with appropriate initial conditions, $\mathbf{u}(\mathbf{x},0) = \mathbf{u}_I(\mathbf{x})$, and boundary conditions, $\mathcal{B}^F(\mathbf{u},p) = 0$. Here, $\mathbf{u} = \mathbf{u}(\mathbf{x},t)$ is the velocity, p the pressure and ν the kinematic viscosity. The term $\alpha\nabla\cdot\mathbf{u}$ in the pressure equation acts as a damping term on the divergence of the velocity. When buoyancy effects are important, an additional temperature equation is added following the Boussinesq approximation as described by Henshaw and Chand (Henshaw and Chand, 2009). The use of LES turbulence models also adds an additional term to the equations. Previously, explicit second- and fourth-order accurate schemes have been developed to solve the equations on overlapping grids (Henshaw, 1994; Henshaw and Petersson, 2003). In this paper we describe the verification and validation of a new approach that combines high-order accurate compact schemes with implicit approximate factorization methods. This new method alleviates the small timestep restriction on high resolution grids imposed by the viscous timescale while preserving the efficiency of explicit finite difference methods.

CgWind also exploits the composite grid approach, which leverages the computational benefits of overlapping, structured grids to represent complex geometry (Chesshire and Henshaw, 1990). These grids are ideal for the high-order accurate compact discretizations used by CgWind as well as the matrix-free geometric multigrid algorithm that enables large-scale, high-resolution computations with realistic geometry (Henshaw, 2005). The memory and CPU performance advantages of high-order accurate methods on structured grids allows CgWind to perform simulations at spatial resolutions currently unobtainable by many other approaches. For example, CgWind's memory footprint for a 3D computation can be as low as $1 - 2Gb$ per million grid points depending on the number of overlapping grids and their topology. Consequently, high-resolution computations can be performed efficiently even on modest workstations and clusters.

Currently there are two subgrid-scale models in CgWind: a simple Smagorinsky style dissipation and a new high-order model more compatible with the resolution properties of CgWind's fourth order spatial discretization. The high-order model relies on a hyperviscosity whose nonlinear coefficient is related to the local strain rate via the smallest scale estimates of Henshaw, Kreiss and Reyna (Henshaw et al., 1989). Other LES turbulence models are currently under development.

3 VERIFICATION

Verification is an essential step in the development of any computational tool. Prior to using a code that approximates a given a set of equations, such as Equation 1, we must ensure that the numerical methods are implemented correctly and that their observed properties (stability and accuracy) match the theory. In the case of CgWind, this verification process tests both the basic numerical method and the complexities related to the moving overlapping grids, multigrid, and boundary conditions.

While it is common to verify numerical methods using simple analytical solutions to the model equations, this approach is often hampered by the approximate nature of such solutions

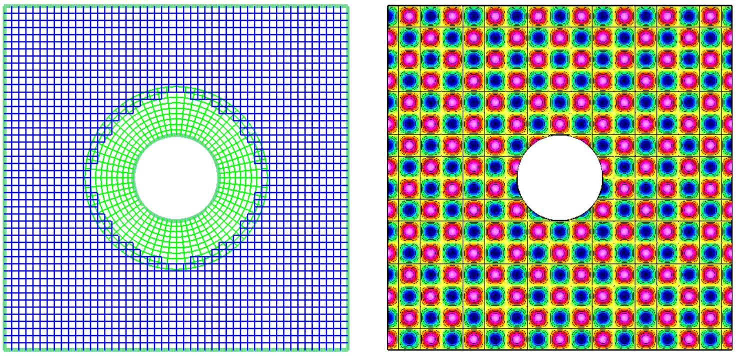

h_{max}	$\lvert e_p \rvert_\infty$	$\lvert e_u \rvert_\infty$	$\lvert e_v \rvert_\infty$	$\lvert \nabla \cdot \mathbf{u} \rvert_\infty$
6.13e-02	1.17e-02	4.35e-03	4.93e-03	9.36e-02
3.08e-02	7.16e-04	1.68e-04	1.72e-04	5.99e-03
1.54e-02	4.31e-05	1.14e-05	9.52e-06	4.45e-04
7.70e-03	2.91e-06	7.62e-07	6.67e-07	3.43e-05
rate	4.0	4.1	4.3	3.8

Figure 1: A two-dimensional overlapping grid (left) and "twilight-zone" (i.e. manufactured) solution (right). Errors and estimated convergence rates for a time dependent exact solution are listed in the table where h is grid spacing and $|e|_\infty$ denotes the maximum error norm. The timestep is reduced by a factor of one-quarter for each resolution so that the time errors scale at the same rate as the spatial errors.

or reduced complexity (i.e. many are one dimensional) needed to arrive at a closed form solution. In both cases, the performance of the numerical method cannot be verified in the presence of complex geometry and full dimensionality of realistic problems. In contrast, the method of twilight-zone, or manufactured, solutions provides a powerful technique for rigorously verifying the implementation of a numerical method in both simple and complex computational domains. In this approach, an exact solution is chosen as a function of space and time, for example

$$\mathbf{u}(\mathbf{x}, t) = \mathbf{c}\cos(\pi f_t t)\sin(\pi f_x x + s_x)\sin(\pi f_y y + s_y)\sin(\pi f_z z + s_z), \tag{2}$$

where $\mathbf{c}$ is a vector of coefficients for each component of the solution vector $\mathbf{u}$. This exact solution for $\mathbf{u}$ can be substituted into the governing equations, and forcing terms can be derived and added to the equations to ensure that $\mathbf{u}$ is an exact solution. The numerical method can then be applied to the governing equations with the appropriate forcing and the computed solution compared to the exact solution. These verification tests ensure that the algorithms are implemented properly and that important properties of the method (e.g. order of accuracy, stability, etc) are preserved. For example, when implementing high-order accurate methods it is easy to introduce coding or algorithmic errors that produce solutions that are consistent but are not of the expected order of accuracy. Rigorous verification via manufactured solutions remains one of the few tools capable of detecting such errors.

Figure 1 illustrates a simple overlapping grid and a manufactured solution on this grid. The table in Figure 1 shows the estimated fourth-order convergence rates for CgWind's algorithms with a $2D$ geometry and manufactured solution. Figure 2 shows pressure contours on cutting planes through a $3D$, time dependent manufactured solution for a cylinder in a box. This grid system consists of two grids: one Cartesian grid for the background and one cylindrical grid for the cylinder. The accompanying table demonstrates the fourth-order accuracy of the numerical method for the full three-dimensional problem.

Moving grid algorithms present their own unique challenges in the context of verification. Boundary conditions that preserve both temporal and spatial accuracy are nontrivial to imple-

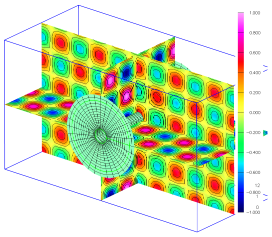

(a) grid and solution

h_{max}	$\lvert e_p\rvert_\infty$	$\lvert e_u\rvert_\infty$	$\lvert e_v\rvert_\infty$	$\lvert e_w\rvert_\infty$	$\lvert\nabla\cdot\mathbf{u}\rvert_\infty$
2.94e+00	5.10e-02	6.71e-02	3.56e-02	3.44e-02	1.52e-01
1.47e+00	3.62e-03	4.40e-03	2.19e-03	2.21e-03	2.28e-02
7.36e-01	2.62e-04	3.16e-04	1.44e-04	2.34e-04	1.34e-03
rate	3.8	3.9	4.0	3.6	3.4

(b) convergence rates

Figure 2: Grid, solution and convergence rates for a 3D verification test.

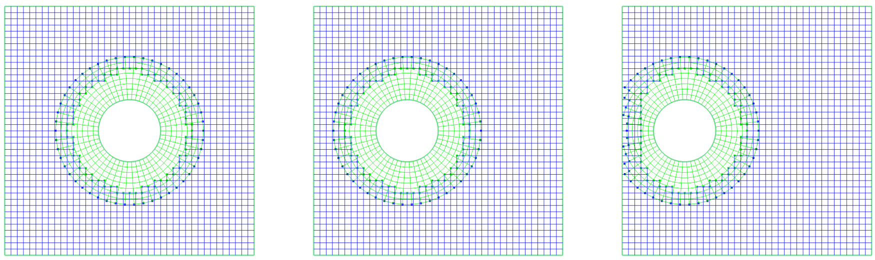

(a) $t = 0.0$ (b) $t = 0.5$ (c) $t = 1.0$

h_{max}	$\lvert e_p\rvert_\infty$	$\lvert e_u\rvert_\infty$	$\lvert e_v\rvert_\infty$	$\lvert\nabla\cdot\mathbf{u}\rvert_\infty$
6.84e-02	8.44e-02	1.80e-01	1.51e-01	1.80e+00
3.44e-02	1.72e-02	2.25e-02	2.61e-02	4.63e-01
1.72e-02	7.92e-03	5.49e-03	5.83e-03	1.54e-01
8.60e-03	2.69e-03	1.10e-03	1.39e-03	5.42e-02
rate	1.6	2.4	2.3	1.7

(d) convergence rates

Figure 3: Manufactured solution based convergence rate estimates for the translating cylinder test case. Currently only 2nd order accurate boundary conditions are implemented for moving grids.

ment as are the algorithms that manage the dynamic grid generation and interpolation required with bodies in relative motion. Nevertheless, the method of manufactured solutions can still be incorporated into the solver to test even this challenging case. While only second-order accurate moving grid boundary conditions have been completed, Figure 3 shows the second-order convergence rates for a translating cylinder and some of the intermediate grids generated during the computation. Note that this calculation can be performed in several ways. For example, the cylinder can remain stationary with the background grid "translating" via boundary conditions specifying the streaming velocity. Alternatively, the background grid can be stationary with zero velocity while the cylinder moves relative to it. Both cases are tested and yield similar results, with the moving cylinder results presented in the table.

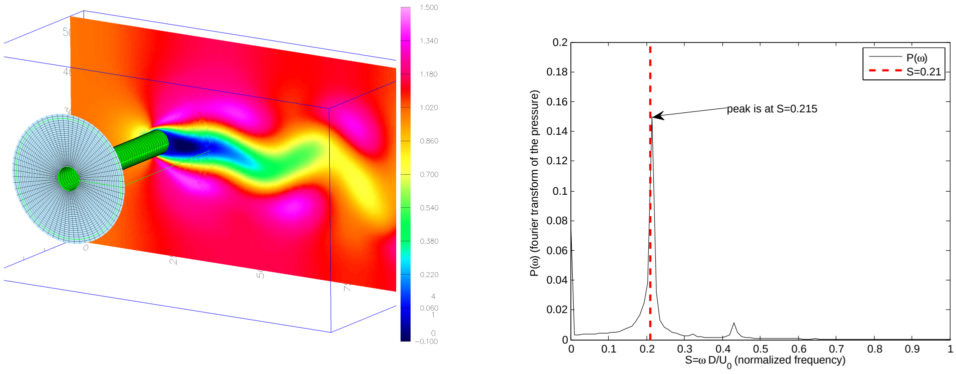

(a) cylinder grid and x-velocity, $t = 700s$

(b) Fourier transform of pressure signal vs nondimensional frequency (Strouhal number)

Figure 4: Reynolds number 1000 Flow past a right circular cylinder. Note the dominant frequency matches the experimentally determined Strouhal number of 0.21 marked by the dashed verticle line.

4 VALIDATION

Once it is verified that a numerical model properly approximates the intended mathematical model, validation can then be performed to demonstrate the suitability of the mathematical model to represent the physical problem of interest. Generally, validation is performed by comparing the numerical results with corresponding experimental data that represent the problems of interest. In this case, CgWind is tested against three cases: the transverse flow past a right circular cylinder, the time dependent flow past an impulsively started rotating cylinder (Coutanceau and Menard, 1985), and the $Re = 12000$ flow past a steep hill (Ishihara et al., 1999). The first test case examines the basic fourth order accurate algorithm's ability to model resolvable (i.e. low Reynolds number) flows. The second case tests the second-order accurate moving grid algorithm. Finally, the third case is more directly relevant to wind engineering and exposes some current limitations of the code.

4.1 3D Flow past a circular cylinder

Figure 4 summarizes the results of a validation test consisting of a right circular cylinder placed in a freestream flow normal to the cylinder axis. The Reynolds number based on the streaming velocity and cylinder diameter is 1000. The inflow velocity is $U_0 = 1$; the outflow condition consists of the equation $p + \delta\frac{\partial p}{\partial n} = 0$ where δ is the length scale for the domain; and the remaining boundaries are slip walls.

The Strouhal number, $St = \frac{\omega D}{U_0}$, was computed and compared to the experimentally determined value of 0.21 (Schlichting, 1979). The flow was simulated to a nondimensional time of 700 and the pressure recorded at a point in the wake 8 diameters downstream of the cylinder. Figure 4 indicates that the dominant Fourier mode of this pressure signal matches the known shedding frequency.

A grid with approximately $400k$ nodes in two components (background and cylinder) was employed. The calculation required less than three hours of computation on six Xeon $2.2Ghz$

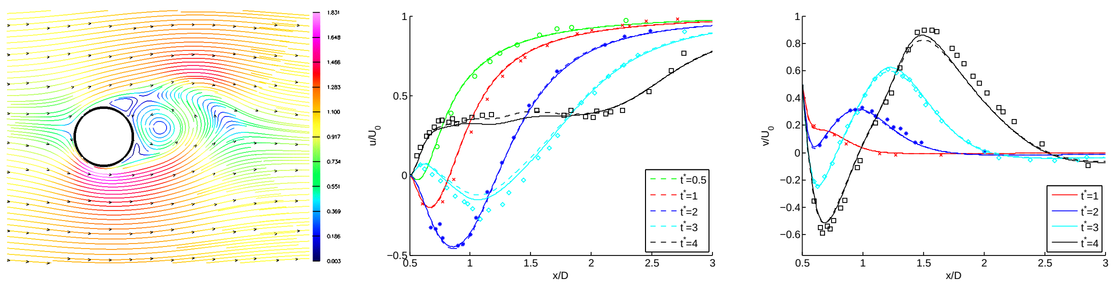

(a) streamlines at t^*=4 (b) x-velocity comparison (c) y-velocity comparison

Figure 5: Streamlines and comparisons with experimental data for the Re=200 flow near an impulsively started rotating and translating cylinder. Solid curves show results for both rotation and translation of the cylinder; dashed lines depict the rotating cylinder with the freestream imposed via boundary conditions; symbols are the experimental data. These results are sensitive to the startup time scale.

processors and approximately $1Gb$ of memory. The minimum amount of memory required per process appears to be approximately $80GM$. Consequently, a single CPU computation actually requires less memory (about $600Mb$); however, such a computation also takes six times longer.

4.2 2D impulsively started rotating cylinder

The Coutanceau and Menard investigation of an impulsively started rotating and translating cylinder provides an excellent validation case for time dependent calculations of bodies in relative motion (Coutanceau and Menard, 1985). This flow is parameterized by the the Reynolds number, $Re = \frac{U_0 D}{\nu} = 200$, the translation velocity, U_0, cylinder diameter, D, and a nondimensional rotation parameter, $\alpha = \frac{\omega D}{2U_0} = 0.5$ with ω as the angular velocity. The low Reynolds number of this flow facilitates adequate spatial resolution, even by CgWind's second-order accurate moving grid discretization. For the comparisons shown, a cubic ramp function was used that start from $U_0 = \alpha = 0$ and reaches the steady state values of $U_0 = 1$,$\alpha = 0.5$ at time 0.1. A $2D$ two grid configuration similar to that shown in figure 1 is used and is adjusted for the dimensions of the problem. The grid contains $368,530$ vertexes, which ensures adequate spatial resolution as determined via grid resolution study.

Figure 5 shows the streamlines at a final nondimensional time of $t^* = \frac{tU_0}{2R} = 4$ as well as comparisons of the two velocity components as a function of distance behind the cylinder for several times. The calculations are performed twice: once with the cylinder rotating and translating (solid lines in the figure), and once with the cylinder rotated while the translation is imposed as boundary conditions on the background grid. As figure 5 indicates, both sets of results are in agreement with the experiment,especially considering the 5% estimated uncertainty in the experimental data.

Despite being 2D and low Reynolds number, this computation is algorithmically complex. At each time step the overlapping grid is adjusted for the rigid body motion, interpolation points are recomputed, and newly exposed points are interpolated.Nevertheless, this calculation was run with $368,530$ grid points, using $177Mb$, and took 747 steps in less than one hour on a single cpu (Intel Xeon 2.2Ghz) time to complete.

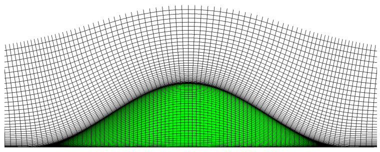

(a) grid near the hill

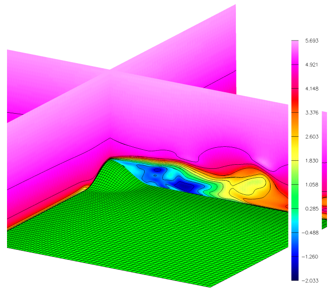

(b) x-velocity contours

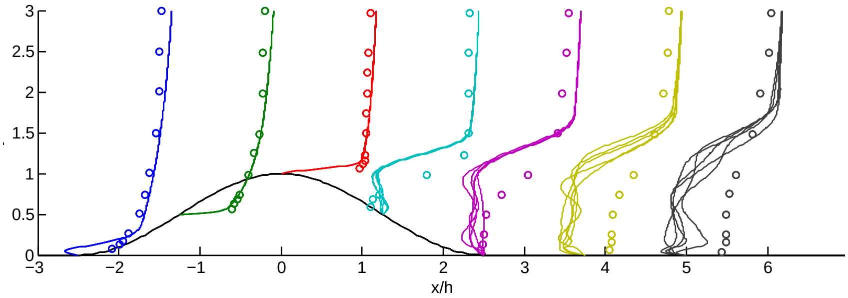

(c) instantaneous u/U_0 (curves) and experimental values (circles)

Figure 6: Grid, x-velocity contours and experimental comparison for the $Re = 12000$ flow past a steep hill. Note that no wall model was used to account for surface roughness probably resulting in the poor agreement.

4.3 3D Steep hill

Ishihara and Hibi, et al. conducted experiments of flow past a model hill with varying surface roughnesses that provide data for validation purposes (Ishihara et al., 1999; Meng and Hibi, 1998). The hill is defined by the profile $z(r) = Hcos^2(\frac{\pi r}{2L})$ for $r \leq L$; $z(r) = 0$ for $r > L$; where $r = \sqrt{x^2 + y^2}$, H is the height of the hill ($40mm$) and $2L$ is the hill's width ($200mm$). The Reynolds number based on the H is approximately 12000. The domain for our calculations consists of a box, centered on the hill, of dimensions $28H$x$25H$x$6H$ in the x, y and z axes respectively. Inflow velocity is given by the power law boundary layer profile provided by Ishihara, Hibi et al, while the hill and lower wall have no-slip (zero velocity) boundaries. The remaining computational boundaries are outflows with a mixed condition on the pressure given by the equation $p + \delta\frac{\partial p}{\partial n} = 0$ where δ is a length scale for each direction.

Figure 6 depicts the results from a calculation with $4x10^6$ grid points on 128 processors. While qualitatively "correct" in some respects, the results do not match the experiment very well, particularly in the wake. However, these results should be studied with the caveat that wall models have not been implemented. Consequently, these comparisons are shown for ill resolved no-slip boundary conditions. The wall grid spacing was eighteen times larger than the experimentally estimated roughness scale. Nevertheless, this spacing resulted in very fine grids near the boundary that, even with the implicit algorithm, required small timesteps and 56 hours of computer time.

We hope to improve on these results by implementing wall models that accurately account for surface roughness. In retrospect, it was optimistic to use this case as an initial validation study due to the aerodynamically rough nature of the flow. A wall model would also obviate the need for such fine grid spacing allowing quicker turn around on such problems. This case also highlighted optimization scaling issues within our algorithms that need to be addressed.

5 STATUS AND FUTURE WORK

CgWind is currently under active development. The verification and initial validation results suggest that the core numerical algorithms are functioning as expected. However, validation tests, such as the steep hill, indicate the need for more work in phenomenological modeling of relevance to wind engineering applications as well as further verification. These verification and validation processes are only the beginning of a continuous effort to ensure that CgWind provides accurate and useful results. We expect to release the current version of the solver in the summer of 2011. An older version, along with documentation, (`cgIns`) can be found at `http://computation.llnl.gov/casc/Overture/`.

6 ACKNOWLEDGMENTS

The authors wish to thank Bill Henshaw for his contributions to the code, algorithms and theory that form the basis of this work. This work was performed under the auspices of the U.S. Department of Energy (DOE) by Lawrence Livermore National Laboratory under Contract DE-AC52-07NA27344, by Laboratory Research and Development funding and by DOE contracts from the ASCR Applied Math Program. LLNL-CONF-483351

REFERENCES

Kyle K. Chand and William D. Henshaw. Overture. Technical Report http://www.llnl.gov/CASC/Overture, Lawrence Livermore National Laboratory, 2007.

Kyle K. Chand, William D. Henshaw, Katherine A. Lundquist, and Michael A. Singer. Cgwind: A high-order accurate simulation tool for wind turbines and wind farms. In *The Fifth International Symposium on Computational Wind Engineering*, 2010.

G. S. Chesshire and W. D. Henshaw. Composite overlapping meshes for the solution of partial differential equations. *J. Comput. Phys.*, 90(1):1–64, 1990.

Madeleine Coutanceau and Christian Menard. Influence of rotation on the near-wake development behind and impulsively started circular cylinder. *Journal of Fluid Mechanics*, 158:399–446, 1985.

William D. Henshaw. A fourth-order accurate method for the incompressible Navier-Stokes equations on overlapping grids. *J. Comput. Phys.*, 113(1):13–25, July 1994.

William D. Henshaw. On multigrid for overlapping grids. *SIAM Journal on Scientific Computing*, 26(5):1547–1572, 2005.

William D. Henshaw and Kyle K. Chand. A composite grid solver for conjugate heat transfer in fluid-structure systems. *J. Comput. Phys.*, 228:3708–3741, 2009.

William D. Henshaw and N. Anders Petersson. A split-step scheme for the incompressible Navier-Stokes equations. In M.M. Hafez, editor, *Numerical Simulation of Incompressible Flows*, pages 108–125. World Scientific, 2003.

William D. Henshaw, H.-O. Kreiss, and L. G. M. Reyna. On the smallest scale for the incompressible Navier-Stokes equations. *Theoretical and Computational Fluid Dynamics*, 1:65–95, 1989.

Takeshi Ishihara, Kazuki Hibi, and Susumu Oikawa. A wind tunnel study of turbulent flow over a three-dimensional steep hill. *Journal of Wind Engineering and Industrial Aerodynamics*, 83:95–107, 1999.

Yan Meng and Kazuki Hibi. An experimental study of turbulent boundary layer over steep hlls. In *15th National Symposium on Wind Engineering*, pages 61–66, 1998.

H. Schlichting. *Boundary-Layer Theory*. McGraw-Hill, New York, 1979. Seventh Edition.